Journal of Computational Physics **160,** 541–563 (2000)
doi:10.1006/jcph.2000.6471, available online at http://www.idealibrary.com on IDEAL®

A Wave Automaton for Wave Propagation in Inhomogeneous Anisotropic Media

Olivier Legrand, Fabrice Mortessagne, Patrick Sebbah, and Christian Vanneste

Laboratoire de Physique de la Matière Condensée, Université de Nice-Sophia Antipolis, Parc Valrose, BP 71, 06108 Nice Cedex 2, France
E-mail: vanneste@unice.fr

Received August 16, 1999; revised February 16, 2000

This paper presents an extension built on a hexagonal grid of the wave automaton, which was introduced in past few years for describing wave propagation in inhomogeneous media. This new method is capable of computing wave propagation in 2D anisotropic media without the need for introducing interpolating schemes. After a comparison of isotropic single scattering with analytical results using Mie theory, the method is used to compute the field scattered by one anisotropic particle for various orientations of its principal axes. Scattering by a collection of anisotropic particles is also presented.

Key Words: wave propagation; time domain; anisotropy.

1. INTRODUCTION

The wave automaton is a numerical method that has been introduced to describe wave propagation in random media [1, 2]. By using appropriate propagation and scattering rules over a discrete lattice, it can be considered as a discrete implementation of Huygens' principle [3]. In particular, it bears strong resemblance with the transmission line matrix modeling (TLM) method, which is commonly used to solve the Maxwell equations in electromagnetic structures [4]. However, it differs from the TLM method in two ways. First, it propagates and scatters real or complex quantities over the network instead of voltage pulses as in TLM. In the following development, we shall refer to these real or complex quantities as currents. Note that it also differs from lattice gas automata that use Boolean variables (see, for instance, the recent model for 3D electromagnetic propagation introduced in [5]). Next, the construction of the wave automaton relies on the fundamental symmetries of the current's dynamics such as time reversal and reciprocity [6, 7]. Due to this construction, the model is entirely determined by a network of unitary scattering matrices. Hence, it also belongs to a large family of similar models used in different areas

0021-9991/00 $35.00

of physics: the lattice Boltzmann wave model [8, 9], quantum cellular automata [10, 11], network models (NWM) [12, 13], etc.

The discrete wave equations resulting from the general construction described in [7] were the Schrödinger, the Klein–Gordon, and the classical wave equations. In this paper, we will focus on this last equation. While this equation allowed the simulation of wave propagation in inhomogeneous media, it was, however, limited to isotropic media. This limitation is also found in usual methods devoted to numerical simulation of wave equations such as Maxwell equations. For instance, the finite-difference time-domain (FDTD) method needs for anisotropic materials the introduction of additional interpolation schemes in order to get field values which are not available from the FDTD grid [14]. Similarly, the problem has been solved with the TLM method by introducing a new generalized TLM node [15]. Since the wave automaton can be identified with a finite-difference algorithm, one could think of introducing interpolation schemes as in the FDTD method. However, this would be in conflict with the spirit of the method, which is founded on an equivalent of Huygens' principle. Propagating current between nodes cannot be associated with such interpolation schemes. It turns out that two of the hypotheses made in the general construction of the isotropic wave automaton must be modified in order to handle anisotropic media. The first one seems natural and consists in abandoning the isotropy of the process that describes the scattering of the currents at the nodes of the network. However, relaxing the isotropy of the scattering process is not sufficient. It turns out that the principal axes of the resulting anisotropic medium are bound to lie along the axes of the Cartesian grid, thus preventing the model from describing an anisotropic material with principal axis along arbitrary directions. This led us to use a hexagonal grid instead of a Cartesian grid. This task is simplified by the fact that most of the results obtained in [7] are valid on any arbitrary lattice. Hence, one just needs to adapt the main steps of the construction described in [7] to the hexagonal lattice.

The paper is organized as follows. In Section 2, we recall briefly the main steps of the construction, which led to the general discrete wave equation described in [7]. This includes the definition of the currents and of the field, the propagation and scattering rules, and their symmetries. We stress the importance of the special form of the scattering matrices, which is needed to close the wave equation. This result enables us to eliminate the currents from the equation that governs the field evolution and makes the wave automaton equivalent to a finite-difference scheme. We conclude by showing that all hypotheses made in [7] lead to modeling an isotropic medium. In Section 3, we abandon some of the hypotheses introduced in Section 2. We deduce in particular the finite-difference version of the wave equation on a hexagonal grid. We show that this equation is appropriate to describe a two-dimensional anisotropic medium with arbitrarily oriented principal axes. In Section 4, we consider an inhomogeneous medium. We focus on the special treatment that is needed to describe the interface separating two different media. In Section 5, we consider the far-field patterns of Mie scatterers to demonstrate the capability of the algorithm. Excellent agreement is found between the wave automaton and exact results for isotropic scatterers. Then, far-field patterns of anisotropic scatterers are presented for which no analytical results are available. In conclusion, we discuss possible extensions of this work.

2. THE WAVE AUTOMATON FOR AN ISOTROPIC MATERIAL

In this section, we recall the definitions, notations, and main steps of the construction of a discrete scalar wave equation in an isotropic medium. The details can be found in [7].

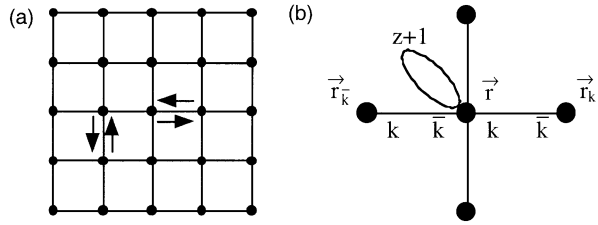

FIG. 1. (a) Propagation of currents along the bonds of a regular lattice. For convenience, a square lattice has been represented. However, most of the results discussed in this section are valid for lattices with arbitrary coordination number z. (b) The bonds are labeled $k = 1; \ldots; z+1$ at each node $\vec{r}$. The neighbor node that is linked to $\vec{r}$ through bond k is called $\vec{r}_k$. As the bonds are labeled in the same manner at each node, note that bond number k at node $\vec{r}$ is given a different number at node $\vec{r}_k$. For notation convenience, we note $\bar{k}$ this number. Hence, bonds k at node $\vec{r}$ and $\bar{k}$ at node $\vec{r}_k$ designate the same bond. With this notation, the propagation step reads $E_{\bar{k}}.\vec{r}_k; t + \Delta/ = S_k.\vec{r}; t/; k = 1; \ldots; z+1$. Note also that for $k = z+1; \vec{r}_{z+1} \equiv \vec{r}$.

The currents are defined as real or complex numbers that propagate along the bonds of a discrete lattice. The nodes of the lattice are labeled by the discrete vector positions $\vec{r}$. Although most of the results described in this section are valid over any arbitrary lattice, we shall consider in the following a regular lattice (i.e., a Bravais lattice) with fixed coordination number z. Moreover since we are only interested in the classical scalar wave equation and not, for instance in the Schrödinger equation, it will be sufficient to consider real currents. At each time $t; z$ outgoing currents $S_k.\vec{r}; t/; k = 1; \ldots; z$ leave each lattice node $\vec{r}$ and propagate in one discrete time step Δ to the z neighbor nodes $\vec{r}_k$, where they become incident currents $E_{\bar{k}}.\vec{r}_k; t + \Delta/$. We have used the following notations. Node $\vec{r}_k$ is the neighbor site, which is linked to node $\vec{r}$ by the bond k, along which the currents $E_k.\vec{r}; t/$ and $S_k.\vec{r}; t/$ propagate. Moreover, bond k for node $\vec{r}$ is referred to as bond $\bar{k}$ for node $\vec{r}_k$ (Fig. 1). With this convention, the propagation step along the bond k of node $\vec{r}$ (or bond $\bar{k}$ of node $\vec{r}_k$) reads $E_{\bar{k}}.\vec{r}_k; t + \Delta/ = S_k.\vec{r}; t/$ and $E_k.\vec{r}; t + \Delta/ = S_{\bar{k}}.\vec{r}_k; t/$. Note that since we consider a Bravais lattice, the index k can be associated to a particular lattice direction and $\bar{k}$ to the opposite direction. This would not be true for a random lattice, as considered, for instance, in [7]. An additional outgoing current $S_{z+1}.\vec{r}; t/$ is attached to each node. This current (hereafter referred to as the on-site current) can be considered as propagating along a loop attached to the node. It becomes an incident current $E_{z+1}.\vec{r}; t + \Delta/$ on the same node at the next time step.

Each node $\vec{r}$ of the lattice is a scatterer described by a matrix that instantaneously transforms the $z+1$ incident currents $E_k.\vec{r}; t/; k = 1; \ldots; z+1$ in $z+1$ outgoing currents $S_k.\vec{r}; t/$. Hence, the scattering process is described by

$$S_k.\vec{r}; t/ = \sum_{l=1}^{z+1} s_{kl}.\vec{r}/E_l.\vec{r}; t/ \qquad k = 1; \ldots; z+1; \tag{2.1}$$

where the $s_{kl}.\vec{r}/$ are the elements of the $.z+1/ \times .z+1/$ scattering matrix S. The time evolution of the currents is summarized in Fig. 2.

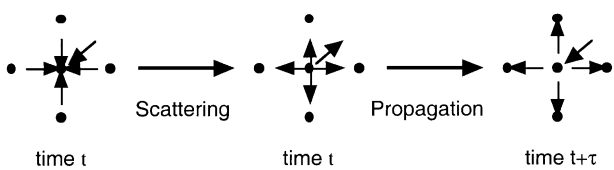

FIG. 2. Scattering and propagation of currents.

The field at node $\vec{r}$ and at time t is defined by a linear combination of the incident currents

$$9.\vec{r};t/ = \sum_{k=1}^{z+1} ,_k.\vec{r}/E_k.\vec{r};t/; \tag{2.2}$$

where the $,_k.\vec{r}/$ are real coefficients to be determined by the properties discussed below.

The most general explicit form of the discrete wave equation, which governs the time evolution of $9.\vec{r};t/$, can be written

$$9.\vec{r};t+¿/ = f.9.\vec{r}';t'/;9.\vec{r}'';t''/;9.\vec{r}''';t'''/;:::/; \tag{2.3}$$

where the field at node $\vec{r}$ and at time $t+¿$ is computed from known values of the field at specific nodes $\vec{r}';\vec{r}'';:::$ and at previous times $t';t''$, etc. By using (2.2), Eq. (2.3) becomes

$$\sum_{k=1}^{z+1} ,_k.\vec{r}/E_k.\vec{r};t+¿/ = f\left(\sum_{k=1}^{z+1} ,_k.\vec{r}'/E_k.\vec{r}';t'/;\sum_{k=1}^{z+1} ,_k.\vec{r}''/E_k.\vec{r}'';t''/;\sum_{k=1}^{z+1} ,_k.\vec{r}'''/E_k.\vec{r}''';t'''/;:::\right): \tag{2.4}$$

It has been established in [7] that this evolution equation of the currents is possible if the elements of the scattering matrix S have the structure

$$s_{kl}.\vec{r}/ = ‰_k.\vec{r}/,_l.\vec{r}/ - „_k.\vec{r}/–_{kl}; \tag{2.5}$$

where the $,_l.\vec{r}/$ are the coefficients introduced in the definition of the field (Eq. (2.2)). $‰_k.\vec{r}/$ and $„_k.\vec{r}/$ are coefficients to be determined and $–_{kl}$ is the Kronecker symbol. Moreover, $„_k.\vec{r}/$ must satisfy the condition

$$\forall k = 1;:::;z+1 \qquad „_k.\vec{r}/„_{\bar{k}}.\vec{r}_k/ = „^2; \tag{2.6}$$

where the constant $„^2$ is independent of the node position $\vec{r}$. Equations (2.5) and (2.6) are essential in the construction of the model and have been named closure conditions in [7]. Without them, it would be impossible to obtain for $9.\vec{r};t/$ a closed equation like (2.3), where no current's term appears.

The construction of the model goes further by introducing fundamental symmetries of the evolution of the currents. The first symmetry is time reversal, which implies that the scattering process is reversible when the directions of the current arrows are reversed. This yields the condition $S^{-1} = S$ for the scattering matrix. The next symmetry is reciprocity. Each matrix element s_{kl} of S describes one elementary current process, which is transmission, reflection or scattering. It couples the two channels (bonds) k and l. Reciprocity means that the scattering process from k to l and the reciprocal process from l to k have the same amplitude. In other words, $\forall k;l = 1;:::;z+1;s_{lk} = s_{kl}$. Thus, the matrix S is symmetrical. Note that the properties $S^{-1} = S$ and $S = S^t$ imply that S is orthogonal.

By using the current propagation and scattering rules, the closure equations (2.5), (2.6), and the two previous symmetries, one obtains

$$9.\vec{r};t+¿/ + 9.\vec{r};t-¿/ = \sum_{k=1}^{z+1} ,_k.\vec{r}/‰_{\bar{k}}.\vec{r}_k/9.\vec{r}_k;t/; \tag{2.7}$$

where

$$\%_k.\vec{r}/ = .1 + 1=„^2/„_k.\vec{r}/, _k.\vec{r}/=3.\vec{r}/ \tag{2.8}$$

$$3.\vec{r}/ = \sum_{k=1}^{z+1} , _k^2.\vec{r}/ \tag{2.9}$$

$$\forall\vec{r}; \quad \forall k = 1;:::;z+1 \qquad „_k^2.\vec{r}/ = „^2 = 1: \tag{2.10}$$

Equation (2.7) is an equation of the type (2.3). This is a closed equation for $9.\vec{r}; t/$, where no current appears explicitly. In the next section, Eq. (2.7) will be the starting point for the construction of the wave equation in an anisotropic medium. However, we continue with the isotropic case in order to point out the hypotheses that are not compatible with anisotropy.

The remaining unknown parameters are the $(z+1)$ coefficients $, _k.\vec{r}/$. To determine the values of these parameters, isotropy of the scattering process has been assumed in [7]. This additional symmetry means that at any node all bonds are equivalent (except the on-site bond). In other words, the scattering matrix is invariant under a new labeling of the bonds. One finds

$$\forall k; l \quad k; l \neq z+1 \qquad , _k.\vec{r}/ = , _l.\vec{r}/: \tag{2.11}$$

Eventually, by considering a d-dimensional Cartesian lattice ($z = 2d$) of lattice constant a, the following discrete wave equation has been obtained in [7]

$$[9.\vec{r}; t + ¿/ + 9.\vec{r}; t - ¿/ - 29.\vec{r}; t/]=¿^2 = , _1.\vec{r}/c_0^2 \left\{ \sum_{k=1}^{2d} [9.\vec{r}_k; t/ - 9.\vec{r}; t/]=a^2 \right\}; \tag{2.12}$$

where $c_0 = a=¿$ is the velocity of the currents, $, _1.\vec{r}/ = 2=.2d + \grave{A}^2.\vec{r}//$ and $\grave{A}.\vec{r}/ = , _{2d+1}.\vec{r}/= , _1.\vec{r}/$. Equation (2.12) is the discretized version of the scalar wave equation

$$@^2 9=@t^2 = c^2.\vec{r}/\nabla^2 9 \tag{2.13}$$

The velocity of the wave is $c^2.\vec{r}/ = 2c_0^2=.2d + \grave{A}^2.\vec{r}//$. Since $c^2.\vec{r}/$ does not depend on the direction of propagation, (2.12) describes an isotropic medium. In reality, there exists a residual anisotropy, which is inherent to any discrete model of wave propagation, even in the case of isotropic wave propagation. It is observed for example in the high frequency range of the dispersion curves $! .\vec{k}/$ that becomes strongly anisotropic when the wavelength is of the order of the lattice constant. Here, $!$ and $\vec{k}$ are the wave frequency and the wave vector, respectively. This effect is well known and thoroughly discussed in several references (see [16–18], for instance). However, we are not interested in that anisotropy, which vanishes in the continuum limit. Therefore, if we want to describe effective anisotropic propagation, some of our previous hypotheses must be modified.

The first guess is to abandon the hypothesis of isotropic scattering. In such a case, one obtains a wave equation with anisotropic propagation. However, one finds that the principal axes are bound to be the coordinate axes of the Cartesian grid. Hence, introducing anisotropic scattering is not sufficient for describing an anisotropic medium whose principal axes are oriented along arbitrary directions.

To make further progress, it is important to notice that the results obtained up to Eq. (2.10) are valid for any arbitrary lattice. In particular, they are not limited to the Cartesian lattice that has been used to obtain Eq. (2.12). Any Bravais lattice in any dimension could have been chosen. Therefore, we may wonder whether another lattice could solve the difficulty encountered with a Cartesian grid. In the next section, we shall see that a hexagonal lattice is a good choice for two-dimensional media.

3. THE WAVE EQUATION IN A TWO-DIMENSIONAL HOMOGENEOUS ANISOTROPIC MEDIUM

We continue the construction of the wave equation starting from equations (2.7)–(2.10) that resulted from the rules governing the current evolution, time reversal symmetry, and reciprocity. In contrast with the previous section, we do not impose isotropic scattering, nor do we impose a Cartesian grid. However, we shall eventually restrict ourselves to a two-dimensional medium.

First, by choosing $\alpha_k(\vec{r}) = \alpha = 1$ and introducing the field $\theta(\vec{r}, t) = \vartheta(\vec{r}, t)/\beta(\vec{r})$, Eq. (2.7) becomes

$$\theta(\vec{r}, t+\Delta t) + \theta(\vec{r}, t-\Delta t) = [2/\beta(\vec{r})] \sum_{k=1}^{z+1} \gamma_k(\vec{r})\, \gamma_{\bar{k}}(\vec{r})\, \theta(\vec{r}_k, t). \tag{3.1}$$

Next, we transform (3.1) in order to write explicitly the second order time and spatial derivatives of $\theta(\vec{r}, t)$. By using the definition (2.9) of $\beta(\vec{r})$ and remembering that $\gamma_{\overline{z+1}}(\vec{r}_{z+1}) \equiv \gamma_{z+1}(\vec{r})$, one easily obtains

$$\begin{aligned}
&\theta(\vec{r}, t+\Delta t) + \theta(\vec{r}, t-\Delta t) - 2\theta(\vec{r}, t) \\
&\quad = [2/\beta(\vec{r})] \left\{ \sum_{k=1}^{z} \gamma_k^2(\vec{r}) [\theta(\vec{r}_k, t) - \theta(\vec{r}, t)] + \sum_{k=1}^{z} \gamma_k(\vec{r}) [\gamma_{\bar{k}}(\vec{r}_k) - \gamma_k(\vec{r})] \theta(\vec{r}_k, t) \right\} \\
&\quad = [2/\beta(\vec{r})] \left\{ \sum_{k=1}^{z=2} \left(\gamma_k^2(\vec{r}) [\theta(\vec{r}_k, t) - \theta(\vec{r}, t)] + \gamma_{\bar{k}}^2(\vec{r}) [\theta(\vec{r}_{\bar{k}}, t) - \theta(\vec{r}, t)] \right) \right. \\
&\qquad \left. + \sum_{k=1}^{z} \gamma_k(\vec{r}) [\gamma_{\bar{k}}(\vec{r}_k) - \gamma_k(\vec{r})] \theta(\vec{r}_k, t) \right\}.
\end{aligned} \tag{3.2}$$

Note that in the last equation the first summation is made over the $z=2$ directions $(k, \bar{k})$ instead of the z bonds k. Assume that $\gamma_{\bar{k}}(\vec{r}) = \gamma_k(\vec{r})$, which means that two opposite bonds of a node are equivalent. This assumption corresponds to local inversion symmetry and is less stringent than isotropic scattering, where all the $\gamma_k(\vec{r})$ but $\gamma_{z+1}(\vec{r})$ are identical. Then, (3.2) becomes

$$\begin{aligned}
&\theta(\vec{r}, t+\Delta t) + \theta(\vec{r}, t-\Delta t) - 2\theta(\vec{r}, t) \\
&\quad = [2/\beta(\vec{r})] \left\{ \sum_{k=1}^{z=2} \gamma_k^2(\vec{r}) [\theta(\vec{r}_k, t) + \theta(\vec{r}_{\bar{k}}, t) - 2\theta(\vec{r}, t)] \right. \\
&\qquad \left. + \sum_{k=1}^{z} \gamma_k(\vec{r}) [\gamma_{\bar{k}}(\vec{r}_k) - \gamma_k(\vec{r})] \theta(\vec{r}_k, t) \right\}.
\end{aligned} \tag{3.3}$$

We recognize in $[8.\vec{r}_k; t/ + 8.\vec{r}_{\bar{k}}; t/ - 28.\vec{r}; t/]$ the discretized form of the second spatial derivative along the direction $.k; \bar{k}/$. Note also that $,_{\bar{k}}.\vec{r}_k/$ has been replaced by $,_k.\vec{r}_k/$ in the second sum. Hence, if the medium is homogeneous $,_k.\vec{r}_k/ = ,_k.\vec{r}/$ and the last term of (3.3) vanishes. The final equation reads

$$[8.\vec{r}; t + ¿/ + 8.\vec{r}; t - ¿/ - 28.\vec{r}; t/]=¿^2 = \sum_{k=1}^{z=2} c_k^2[8.\vec{r}_k; t/ + 8.\vec{r}_{\bar{k}}; t/ - 28.\vec{r}; t/]=a^2; \tag{3.4}$$

where the velocities

$$c_k^2 = 2c_0^2,_k^2=3 \tag{3.5}$$

do not depend on $\vec{r}$ in a homogeneous medium. As before $c_0 = a=¿$ is the velocity of the currents.

Until now, these results are valid for any lattice. Let us consider first a two-dimensional Cartesian grid with coordinate axes $x; y$. The coordination number is $z = 4$ and (3.4) becomes

$$\begin{aligned}[8.\vec{r}; t + ¿/ + 8.\vec{r}; t - ¿/ - 28.\vec{r}; t/]=¿^2 \\ = c_x^2[8.\vec{r} + -\vec{x}; t/ + 8.\vec{r} - -\vec{x}; t/ - 28.\vec{r}; t/]=a^2 \\ + c_y^2[8.\vec{r} + -\vec{y}; t/ + 8.\vec{r} - -\vec{y}; t/ - 28.\vec{r}; t/]=a^2:\end{aligned} \tag{3.6}$$

Equation (3.6) describes an anisotropic medium. However, the principal axes are aligned along the coordinate axes $x; y$.

Let us consider next a hexagonal lattice with coordinate axes $u; v; w$ (Fig. 3). The coordination number is $z = 6$, and (3.4) becomes

$$\begin{aligned}&[8.\vec{r}; t + ¿/ + 8.\vec{r}; t - ¿/ - 28.\vec{r}; t/]=¿^2 \\ &= c_u^2[8.\vec{r} + -\vec{u}; t/ + 8.\vec{r} - -\vec{u}; t/ - 28.\vec{r}; t/]=a^2 + c_v^2[8.\vec{r} + -\vec{v}; t/ + 8.\vec{r} - -\vec{v}; t/ \\ &\quad - 28.\vec{r}; t/]=a^2 + c_w^2[8.\vec{r} + -\vec{w}; t/ + 8.\vec{r} - -\vec{w}; t/ - 28.\vec{r}; t/]=a^2;\end{aligned} \tag{3.7}$$

where $c_u \equiv c_1 = c_6; c_v \equiv c_2 = c_5$, and $c_w \equiv c_3 = c_4$ according to the labeling of the bonds shown in Fig. 3c. It turns out that Eq. (3.7) is appropriate to describe anisotropic propagation with arbitrarily oriented principal axes.

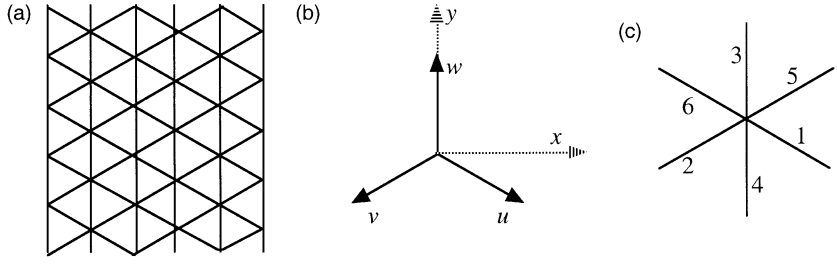

FIG. 3. (a) Hexagonal lattice. (b) The coordinate axes $u; v; w$ are chosen along the three directions of the lattice. (c) Labeling of the bonds at each node of the lattice. With our previous notations, $6 \equiv \bar{1}; 5 \equiv \bar{2}$, and $4 \equiv \bar{3}$.

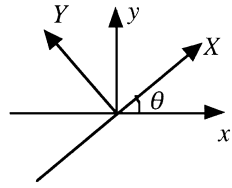

FIG. 4. The direction of the principal axes $X; Y$ is given by μ.

Let us consider a medium with principal axes $X; Y$ making an angle μ with respect to axes $x; y$ (Fig. 4). The wave equation, which reads in the $X; Y$ coordinate system

$$@^2 `=@t^2 = c_X^2 @^2 `=@X^2 + c_Y^2 @^2 `=@Y^2 \tag{3.8}$$

becomes, in the $x; y$ coordinate system,

$$@^2 8=@t^2 = a@^2 8=@x^2 + b@^2 8=@y^2 + c@^2 8=@x@y; \tag{3.9}$$

with

$$\begin{aligned} a &= \left[c_X^2.1 + \cos 2\mu/ + c_Y^2.1 - \cos 2\mu/\right]/2 \\ b &= \left[c_X^2.1 - \cos 2\mu/ + c_Y^2.1 + \cos 2\mu/\right]/2 \\ c &= \left(c_X^2 - c_Y^2\right)\sin 2\mu: \end{aligned}$$

This is precisely the mixed derivative $@^2 8=@x@y$, which prevented Eq. (3.6) from describing anisotropy with arbitrary orientation.

In contrast, it is straightforward to establish that (3.8) becomes in the $u; v; w$ coordinate system

$$@^2 8=@t^2 = fi_u @^2 8=@u^2 + fi_v @^2 8=@v^2 + fi_w @^2 8=@w^2; \tag{3.10}$$

where

$$fi_k = \left[\left(c_X^2 + c_Y^2\right) - 2\left(c_X^2 - c_Y^2\right)\sin\left(\mu_k + 2\mu\right)\right]/3 \qquad k = u; v; w \tag{3.11}$$

Here, μ_k is the angle of axis k with respect to axis x; i.e., $\mu_u = -\ldots=6$, $\mu_v = 7\ldots=6$, and $\mu_w = \ldots=2$.

It is obvious that (3.10) is the continuum limit of (3.7). Therefore, by identifying the fi_k's in (3.10) with the c_k^2's in (3.7) and using (3.5), one obtains

$$,_k^2 = \left(3=6c_0^2\right)\left[\left(c_X^2 + c_Y^2\right) - 2\left(c_X^2 - c_Y^2\right)\sin.\mu_k + 2\mu/\right] \qquad k = 1; 2; 3 \tag{3.12}$$

Remembering that $,_{\bar{k}} = ,_k$ and the definition (2.9) of $3.\vec{r}/$, which becomes for a hexagonal lattice

$$3 = \sum_{k=1}^{7} ,_k^2 = 2\left(,_1^2 + ,_2^2 + ,_3^2\right) + ,_7^2; \tag{3.13}$$

the three equations (3.12) are implicit equations for the $,_k$'s. To find explicit expressions as functions of the physical parameters $c_X; c_Y$, and μ, let us first notice that the $,_k$'s are defined modulo a constant factor in the definition of the field (2.2). In particular, we can express the $,_k$'s by their ratios $,_k^2=,_1^2$, where the scaling factor has been arbitrarily chosen equal to $,_1$. From (3.12) and (3.13), one finds

$$,_k^2 = ,_1^2\left[\left(c_X^2+c_Y^2\right)-2\left(c_X^2-c_Y^2\right)\sin.\mu_k+2\mu/\right]/\left[\left(c_X^2+c_Y^2\right)-2\left(c_X^2-c_Y^2\right)\sin.\mu_1+2\mu/\right] \qquad k=2;3 \quad (3.14)$$

$$,_7^2 = 6,_1^2\left[c_0^2-\left(c_X^2+c_Y^2\right)\right]/\left[\left(c_X^2+c_Y^2\right)-2\left(c_X^2-c_Y^2\right)\sin.\mu_1+2\mu/\right] \quad (3.15)$$

$$3 = 6,_1^2c_0^2/\left[\left(c_X^2+c_Y^2\right)-2\left(c_X^2-c_Y^2\right)\sin.\mu_1+2\mu/\right]: \quad (3.16)$$

If the value of $,_1$ is chosen arbitrarily, the three above expressions are functions of $c_X; c_Y$, and μ. However, it is possible to choose the value of $,_1$ in such a manner that $,_7$ does not depend on the angle μ. To explain this choice, it is useful to understand the role played by $,_7$. Let us consider the special case of isotropic propagation. Then $c_X=c_Y$ and all $,_k$'s but $,_7$ are equal, say $,_k=,_1$, $\forall k=2;:::;6$. Using those conditions (3.12) leads to

$$c_X^2=c_Y^2=3c_0^2/\left(6+,_7^2/,_1^2\right): \quad (3.17)$$

This expression shows that the velocity of the wave is determined by $,_7$. In particular, the maximum wave velocity $c_{\max}^2$ is obtained for $,_7=0$ and is given by

$$c_{\max}=c_0=\sqrt{2}:$$

This result is intuitive. The role played by the on-site current is to trap a fraction of the wave at each node and at each time step. This trapping effect is controlled by the value of $,_7$. The net result is to slow down the wave when $,_7$ increases.

In the anisotropic case, $,_7$ plays a similar role. It is natural to consider that $,_7$ must control the values of the velocities c_X and c_Y independently of the orientation μ. This condition will be fulfilled if μ does not appear in Eq. (3.15). Hence, $c_X; c_Y$, and μ being given, we make the choice

$$,_1^2=\left[\left(c_X^2+c_Y^2\right)-2\left(c_X^2-c_Y^2\right)\sin.\mu_1+2\mu/\right]/3c_0^2: \quad (3.18)$$

Using (3.18), one finds

$$,_k^2=\left[\left(c_X^2+c_Y^2\right)-2\left(c_X^2-c_Y^2\right)\sin.\mu_k+2\mu/\right]/3c_0^2 \qquad k=1;2;3 \quad (3.19)$$

$$,_7^2=2\left[1-\left(c_X^2+c_Y^2\right)/c_0^2\right] \quad (3.20)$$

$$3=2: \quad (3.21)$$

We note that (3.20) is the extension to anisotropic media of (3.17), which is only valid for isotropic media. At this stage, the construction of the model is completed. The values of $,_k$ being known and remembering the choice $„_k=„=1$, Eq. (2.8) leads to $‰_k=,_k$. Then, we deduce the elements s_{kl} of the scattering matrix S from (2.5).

Let us point out a limitation of the present model. Notice that Eq. (3.19) determines the square value of $,_k$. Hence, the right-hand side must be positive whatever the orientation μ.

This implies the restriction

$$1/3 \leq c_Y^2/c_X^2 \leq 3; \tag{3.22}$$

or in terms of the indices $n_X = c_{\max}/c_X$; $n_Y = c_{\max}/c_Y$,

$$1/\sqrt{3} \leq n_Y/n_X \leq \sqrt{3}.$$

To conclude the present section, we recall that we have considered a homogeneous medium in our construction. We shall focus on the description of inhomogeneous media in the next section.

4. TWO-DIMENSIONAL INHOMOGENEOUS ANISOTROPIC MEDIA

Let us consider the interface between two different homogeneous media (Fig. 5). Both media are characterized by their values c_X; c_Y; μ and c'_X; c'_Y; μ'. Inside each medium, wave propagation is described by the general equation (3.4). Our task is to identify the steps of our construction, which must be modified to take the interface into account. In Section 4.1, we establish the new equation that governs the time evolution of the field at a node that belongs to the interface. In this new equation, the values of parameters of the wave automaton depend on the way the velocity gradients are described at the interface. This description can be intricate except if simplifying assumptions are used as discussed in Section 4.2.

4.1. Wave Equation at the Interface

We must start from Eq. (3.2), which we rewrite below for a hexagonal lattice:

$$\begin{aligned} &\Psi(\vec{r}; t+\Delta t) + \Psi(\vec{r}; t-\Delta t) - 2\Psi(\vec{r}; t) \\ &\quad = [2/3]\left\{ \sum_{k=1}^{3} \left(\gamma_k^2 [\Psi(\vec{r}_k; t) - \Psi(\vec{r}; t)] + \gamma_{\bar{k}}^2 [\Psi(\vec{r}_{\bar{k}}; t) - \Psi(\vec{r}; t)] \right) \right. \\ &\qquad \left. + \sum_{k=1}^{6} \gamma_k [\gamma_{\bar{k}} \Psi(\vec{r}_{\bar{k}}) - \gamma_k \Psi(\vec{r})] \Psi(\vec{r}_k; t) \right\}. \end{aligned} \tag{4.1}$$

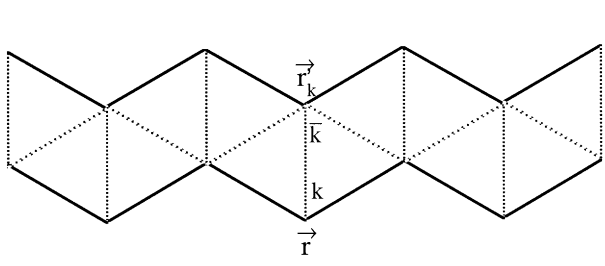

FIG. 5. The dotted lines represent the bonds of the hexagonal lattice, which connect the nodes of two different media. A position vector is denoted $\vec{r}$ in medium 1 and $\vec{r}'$ in medium 2.

Two assumptions have been necessary to obtain Eq. (3.4) for a homogeneous medium. First, we have assumed local inversion symmetry

$$,_{\bar{k}}.\vec{r}/ = ,_k.\vec{r}/ \tag{4.2}$$

and next, homogeneity

$$,_k.\vec{r}_k/ = ,_k.\vec{r}/: \tag{4.3}$$

In particular, both assumptions were necessary to cancel the last term in (4.1). If at the interface $,_k.\vec{r}/$ and $,'_{\bar{k}}.\vec{r}'_k/$ have the values given by Eqs. (3.19) for their respective homogeneous medium they will not be identical in general. Here, we use the prime sign (see Fig. 5) to indicate that $\vec{r}$ and $\vec{r}'_k$ do not belong to the same medium. Hence, the last term in (4.1) will be different from zero. We may wonder whether this could be the interface term that is needed for the inhomogeneous case. It turns out that this guess is not correct. To see this, consider the particular case where $\mu = 0$, $c'_X = c_X$, and $c'_Y \neq c_Y$. The values of $,_k.\vec{r}/$ and $,'_k.\vec{r}'/$ are given by (3.19)

$$,^2_k.\vec{r}/ = \left[\left(c_X^2 + c_Y^2\right) - 2\left(c_X^2 - c_Y^2\right)\sin.\mu_k/\right]/3c_0^2 \qquad k = 1; 2; 3 \tag{4.4}$$

$$,'^2_k.\vec{r}'/ = \left[\left(c_X^2 + c'^2_Y\right) - 2\left(c_X^2 - c'^2_Y\right)\sin.\mu_k/\right]/3c_0^2 \qquad k = 1; 2; 3: \tag{4.5}$$

Consider a plane wave propagating along the x direction, $\mathcal{B}.\vec{r}; t/ = \mathcal{B}_0 \exp i.\,!\,t - kx/$, where $\mathcal{B}_0$ does not depend on y. According to the assumption $c'_X = c_X$, this wave should propagate with velocity c_X in both media. It should not feel the interface and should propagate as in a homogeneous medium. However, since $c'_Y \neq c_Y$, (4.4) and (4.5) imply that $,'_{\bar{k}}.\vec{r}'_k/ \neq ,_k.\vec{r}/$ and the last term in (4.1) is different from zero at the interface. Hence, this term will induce spurious instead of zero scattering.

To avoid this problem, we assume that the equality $,_{\bar{k}}.\vec{r}_k/ = ,_k.\vec{r}/$, which results from (4.2) and (4.3) in a homogeneous medium, is also true at the interface. Hence, the last term in (4.1) always vanishes. However, since in general $,_k.\vec{r}/$ and $,'_k.\vec{r}'_k/$ are different at the interface, this assumption is not compatible with (4.2). Therefore, we shall not postulate local inversion symmetry at the interface. From a physical point of view, this sounds reasonable since inversion symmetry is certainly lost at any interface.

Let us introduce some notation. If $\vec{r}$ and $\vec{r}'_k$ are two nodes connected by bond k at the interface, we note $,_I.\vec{r}; \vec{r}'_k/$ the common value of $,_k.\vec{r}/$ and $,_{\bar{k}}.\vec{r}'_k/$ according to the above hypothesis

$$,_I.\vec{r}; \vec{r}'_k/ = ,_k.\vec{r}/ = ,_{\bar{k}}.\vec{r}'_k/: \tag{4.6}$$

Also, since $,_k.\vec{r}/$ does not depend on $\vec{r}$ inside each homogeneous medium, we note $,_k.\vec{r}/ = ,_k$ in medium 1 and $,_k.\vec{r}'/ = ,'_k$ in medium 2. For instance, with these notations Eq. (4.1) inside medium 1 becomes

$$\mathcal{B}.\vec{r}; t + ¿/ + \mathcal{B}.\vec{r}; t - ¿/ - 2\mathcal{B}.\vec{r}; t/ = \sum_{k=1}^{3} ,^2_k[\mathcal{B}.\vec{r}_k; t/ + \mathcal{B}.\vec{r}_{\bar{k}}; t/ - 2\mathcal{B}.\vec{r}; t/]: \tag{4.7}$$

Here, the $,_k$'s are given by (3.19) and we have used (3.21). At a node $\vec{r}$ of the interface, Eq. (4.1) becomes

$$\begin{aligned}&8.\vec{r};t+¿/+8.\vec{r};t-¿/-28.\vec{r};t/\\&=[2=3.\vec{r}/]\left\{\sum_{k=1}^{6-n},_k^2[8.\vec{r}_k;t/-8.\vec{r};t/]+\sum_{k=1}^{n},_I^2.\vec{r};\vec{r}_k'/[8.\vec{r}_k';t/-8.\vec{r};t/]\right\};\end{aligned}\tag{4.8}$$

where we have separated the n bonds, which connect $\vec{r}$ to medium 2 from the other bonds. Note that we should have written $n.\vec{r}/$ instead of n, since this number depends on the local configuration of node $\vec{r}$. To simplify the notations, we shall keep writing n in the following. The coefficient $3.\vec{r}/$ reads

$$3.\vec{r}/=\sum_{k=1}^{6-n},_k^2+\sum_{k=1}^{n},_I^2.\vec{r};\vec{r}_k'/+,_7^2.\vec{r}/:\tag{4.9}$$

Using $,_{\bar{k}}^2=,_k^2$ in each homogeneous medium, we can rewrite (4.8) as

$$\begin{aligned}&8.\vec{r};t+¿/+8.\vec{r};t-¿/-28.\vec{r};t/\\&=[2=3.\vec{r}/]\left\{\sum_{k=1}^{3},_k^2[8.\vec{r}_k;t/+8.\vec{r}_{\bar{k}};t/-28.\vec{r};t/]\right.\\&\left.+\sum_{k=1}^{n}\left[,_I^2.\vec{r};\vec{r}_k'/-,_k^2\right][8.\vec{r}_k';t/-8.\vec{r};t/]\right\}:\end{aligned}\tag{4.10}$$

We could also write equivalent equations at the nodes $\vec{r}'$ of medium 2 that belong to the interface. In particular, (4.9) becomes

$$3'.\vec{r}'/=\sum_{k=1}^{6-n'},'^2_k+\sum_{k=1}^{n'},_I^2.\vec{r}_k;\vec{r}'/+,'^2_7.\vec{r}'/;\tag{4.11}$$

where n' is the number of bonds which connect $\vec{r}'$ to medium 1.

Finally, we note that $3=2$ in medium 1 and in medium 2 as in any homogeneous medium. There is no special reason for 3 to have a different value at the interface. Therefore, we assume

$$3.\vec{r}/=3'.\vec{r}'/=2;\tag{4.12}$$

a choice to be validated below.

Using (4.12), (4.10) becomes

$$\begin{aligned}&8.\vec{r};t+¿/+8.\vec{r};t-¿/-28.\vec{r};t/]=¿^2\\&=c_0^2\left\{\sum_{k=1}^{3},_k^2[8.\vec{r}_k;t/+8.\vec{r}_{\bar{k}};t/-28.\vec{r};t/]\right.\\&\left.+\sum_{k=1}^{n}\left[,_I^2.\vec{r};\vec{r}_k'/-,_k^2\right][8.\vec{r}_k';t/-8.\vec{r};t/]\right\}\Big/a^2:\end{aligned}\tag{4.13}$$

The first sum in (4.13) is the Laplacian in medium 1. Hence, the last term must be interpreted as a source term due to the interface. To check this, let us consider again the special case of an isotropic medium, i.e., $\forall k = 1;:::;6;\ ,^2_k = ,^2_1$. The last sum in (4.13) becomes

$$\sum_{k=1}^{n} \left[,^2_I.\vec{r};\vec{r}'_k/ - ,^2_k\right][\delta.\vec{r}'_k;t/ - \delta.\vec{r};t/] = \sum_{k=1}^{n} \left[,^2_I.\vec{r};\vec{r}'_k/ - ,^2_1\right][\delta.\vec{r}'_k;t/ - \delta.\vec{r};t/]$$

$$= \sum_{k=1}^{n} \left[,^2_I.\vec{r};\vec{r}'_k/ - ,^2_1\right][\delta.\vec{r}'_k;t/ - \delta.\vec{r};t/] + \sum_{j=1}^{6-n} \left[,^2_j - ,^2_1\right][\delta.\vec{r}_j;t/ - \delta.\vec{r};t/]: \tag{4.14}$$

In the second equality, the last term, which equals zero, has been added on purpose to obtain a summation over all neighbors of node $\vec{r}$. As $,^2_I.\vec{r};\vec{r}'_k/$ is unknown, let us assume

$$,^2_I.\vec{r};\vec{r}'_k/ = \phi,^2_1 + [1-\phi],'^2_k: \tag{4.15}$$

Then, (4.14) reads

$$\sum_{k=1}^{n} \left[,^2_I.\vec{r};\vec{r}'_k/ - ,^2_k\right][\delta.\vec{r}'_k;t/ - \delta.\vec{r};t/]$$

$$= .1-\phi/\left\{\sum_{k=1}^{n} \left[,'^2_k - ,^2_1\right][\delta.\vec{r}'_k;t/ - \delta.\vec{r};t/] + \sum_{j=1}^{6-n} \left[,^2_j - ,^2_1\right][\delta.\vec{r}_j;t/ - \delta.\vec{r};t/]\right\}: \tag{4.16}$$

For a hexagonal lattice, the sum over all neighbors is the discrete form of the quantity $3\vec{\nabla},^2.\vec{r}/\cdot\vec{\nabla}\delta.\vec{r};t/$. Using (3.19) for an isotropic medium, the wave velocity is $c^2 = c_X^2 = c_Y^2 = .3=2/c_0^2,^2_1$. Hence, the last term in (4.13) is the second order discrete approximation of the product $2.1-\phi/\vec{\nabla}c^2.\vec{r}/\cdot\vec{\nabla}\delta.\vec{r};t/$. If we choose $\phi = 0{:}5$, we obtain exactly $\vec{\nabla}c^2.\vec{r}/\cdot\vec{\nabla}\delta.\vec{r};t/$. This last product is known to appear, for instance, in the sound wave equation in the presence of a sound velocity gradient. This indicates that our hypotheses (4.6) and (4.12) have a sound basis. Note that using (4.15), we would have obtained the product $2\phi\vec{\nabla}c^2.\vec{r}'/\cdot\vec{\nabla}\delta.\vec{r}';t/$ for a node $\vec{r}'$ of medium 2. This is also equal to $\vec{\nabla}c^2.\vec{r}'/\cdot\vec{\nabla}\delta.\vec{r}';t/$ when $\phi = 0{:}5$. Actually, we shall see later that the value of ϕ is not essential.

If the velocity is anisotropic, the last sum in (4.13) can be considered as the discrete equivalent for an anisotropic medium of the product $\vec{\nabla}c^2.\vec{r}/\cdot\vec{\nabla}\delta.\vec{r};t/$. It is obvious that such a term will not induce spurious scattering as in the example we considered at the beginning of this section.

4.2. Determination of the Interface Parameters

In (4.9)–(4.11), the parameters $,_I.\vec{r};\vec{r}'_k/;\ ,_I.\vec{r}_k;\vec{r}'/,\ ,_7.\vec{r}/$ and $,'_7.\vec{r}'/$ are unknown. Using (3.13) in both homogeneous media and (4.12), Eqs. (4.9) and (4.11) become

$$,^2_7.\vec{r}/ - ,^2_7 + \sum_{k=1}^{n}\left(,^2_I.\vec{r};\vec{r}'_k/ - ,^2_k\right) = 0 \tag{4.17}$$

$$,'^2_7.\vec{r}'/ - ,'^2_7 + \sum_{k=1}^{n'}\left(,^2_I.\vec{r}_k;\vec{r}'/ - ,'^2_k\right) = 0: \tag{4.18}$$

If N_n and N_b are respectively the numbers of nodes and bonds that belong to the interface, (4.17) and (4.18) form a system of N_n equations, one for each node $\vec{r}$ and $\vec{r}'$. There are first N_n unknown parameters, $,^{2}_{7}.\vec{r}/$ and $,^{\prime 2}_{7}.\vec{r}'/$. Next, remember that $,^{2}_{I}.\vec{r};\vec{r}'_k/ = ,^{2}_{I}.\vec{r}_j;\vec{r}'/$ when $.\vec{r};\vec{r}'_k/$ and $.\vec{r}_j;\vec{r}'/$ correspond to the same bond. Hence, the number of unknown parameters $,^{2}_{I}.\vec{r};\vec{r}'_k/$ or $,^{2}_{I}.\vec{r}_j;\vec{r}'/$ is N_b. Eventually, (4.17) and (4.18) form a linear system of N_n equations with $.N_n + N_b/$ unknown parameters. As $N_b \approx N_n$, these parameters are largely undetermined.

To solve this system, additional constraints are needed. First, nothing prevents us from writing

$$,^{2}_{I}.\vec{r};\vec{r}'_k/ = fi_k.\vec{r};\vec{r}'_k/,^{2}_{k} + [1 - fi_k.\vec{r};\vec{r}'_k/],^{\prime 2}_{k}; \tag{4.19}$$

which is more general than (4.15). The $fi_k.\vec{r};\vec{r}'_k/$ are to be determined. The only hypothesis made in writing (4.19) is that $,^{2}_{I}.\vec{r};\vec{r}'_k/ = ,^{2}_{k}$ if $,^{2}_{k} = ,^{\prime 2}_{k}$. An equation similar to (4.19) can be written for $,^{2}_{I}.\vec{r}_k;\vec{r}'/$. Hence, (4.17) and (4.18) become

$$,^{2}_{7}.\vec{r}/ = ,^{2}_{7} + \sum_{k=1}^{n}[1 - fi_k.\vec{r};\vec{r}'_k/]D_k \tag{4.20}$$

$$,^{\prime 2}_{7}.\vec{r}'/ = ,^{\prime 2}_{7} - \sum_{k=1}^{n'} fi_k.\vec{r}_k;\vec{r}'/D_k; \tag{4.21}$$

where the D_k are known quantities defined as

$$D_k = ,^{2}_{k} - ,^{\prime 2}_{k}: \tag{4.22}$$

We are free to choose the values of $fi_k.\vec{r};\vec{r}'_k/$ for each bond $.\vec{r};\vec{r}'_k/$. This choice being made, (4.20) and (4.21) provide the values of $,^{2}_{7}.\vec{r}/$ and $,^{\prime 2}_{7}.\vec{r}'/$ at each node $\vec{r}$ and $\vec{r}'$ of the interface. To choose the $fi_k.\vec{r};\vec{r}'_k/$, one just has to make sure that the conditions

$$0 \leq ,^{2}_{7}.\vec{r}/; ,^{\prime 2}_{7}.\vec{r}'/ \leq 2 \tag{4.23}$$

are verified. This is a consequence of $3.\vec{r}/ = 3'.\vec{r}'/ = 2$.

However, proceeding that way is not necessary. It means that we are describing in detail the velocity gradient at each bond of the interface. This is generally useless. As a reasonable choice, we can decide that $fi_k.\vec{r};\vec{r}'_k/ = fi_k$. Here the value fi_k depends on the direction $.k;\overline{k}/$ of the hexagonal lattice but does not depend on the particular bond $.\vec{r};\vec{r}'_k/$. Hence, instead of N_n equations, the system (4.20), (4.21) reduces to N_c equations, where N_c is the number of local configurations involving n or n' connecting bonds. Apart from the case where media 1 or 2 correspond to localized defects including a few nodes, N_c is usually much smaller than N_n.

One further approximation is to give to fi_k a unique value $fi_k = fi$ at any bond of the interface, as we did in the isotropic case. Equations (4.20) and (4.21) become

$$,^{2}_{7}.\vec{r}/ = ,^{2}_{7} + [1 - fi]\sum_{k=1}^{n} D_k \tag{4.24}$$

$$,^{\prime 2}_{7}.\vec{r}^{\prime}/ = ,^{\prime 2}_{7} - fi \sum_{k=1}^{n^{\prime}} D_k: \tag{4.25}$$

For instance, if we choose $fi = 1$, we obtain

$$,^{2}_{7}.\vec{r}/ = ,^{2}_{7} \tag{4.26}$$

$$,^{\prime 2}_{7}.\vec{r}^{\prime}/ = ,^{\prime 2}_{7} - \sum_{k=1}^{n^{\prime}} D_k: \tag{4.27}$$

This choice means that the velocity gradients are localized at the nodes $\vec{r}^{\prime}$ of the interface, i.e., at the boundary of medium 2. For the opposite choice, $fi = 0$, the velocity gradients would be concentrated at the medium 1 side. One could also select any intermediate choice $0 < fi < 1$. It is obvious that the chosen value is not important if the thickness of the interface, which is one lattice bond, is much smaller than other characteristic lengths of the system under investigation. Note also that its is possible to describe thicker interfaces by building velocity gradients over several bonds using the same general arguments. Eventually, let us point out again that the choice of fi in (4.24) and (4.25) is limited by the condition (4.23). In Section 5, (4.24) and (4.25) have been used to describe the boundaries of scatterers immersed in a homogeneous medium.

4.3. Summary of the Method

Before providing numerical examples to demonstrate the capability of the wave automation, it is useful to give a short summary of the method. We consider a system made of several anisotropic media labeled by superscripts $M = A; B; C$. Each medium M is characterized by its principal axes X^M, Y^M making an angle μ^M with respect to axes $x; y$ of a two-dimensional Cartesian grid. The wave velocities along X^M and Y^M are c_X^M and c_Y^M, respectively. The special case of an isotropic medium is automatically included when $c_Y^M = c_X^M$.

After the implementation of the geometrical configuration over a triangular lattice, the subsequent step is to associate a scattering matrix to each node of the grid. We proceed in two steps. First, each medium M is considered separately from the others. Next, nodes located at the boundaries between two different media M and N are considered.

Let us consider first any medium M. The only parameters to be calculated are the coefficients $,^M_k;\ k = 1; : : : ; 7$ as a function of $\mu^M; c_X^M$, and c_Y^M according to (3.19) and (3.20). We recall that μ_k, $k = 1; 2; 3$ in (3.19) is the angle of axis k of the triangular grid with respect to axis x. In fact, as inside each homogeneous medium local inversion is obeyed, i.e., $,^{\underline{M}}_{k} \equiv ,^M_k$, only four distinct values of $,^M_k$ are needed. The coefficients $,^M_k$ first enter the definition of the field $9.\vec{r}; t/ = \sum_{k=1}^{7} ,^M_k.\vec{r}/E_k.\vec{r}; t/$ (Eq. (2.2)) and completely determine the scattering elements $s^M_{kl}.\vec{r}/ = \%^M_k.\vec{r}/, ^M_l.\vec{r}/ - \,„^M_k.\vec{r}/-_{kl}$ of the scattering matrix at node $\vec{r}$ (Eq. (2.5)) since $\%^M_k.\vec{r}/ = ,^M_k.\vec{r}/$ and $„^M_k.\vec{r}/ = 1$. At this stage, the coefficients $,^M_k$ are associated to each node of medium M, including the nodes of its boundaries. Hence, as all nodes are identical inside M, it is sufficient to store four values $,^M_k$ for each medium M.

Next, let us consider the interface between two media M and N. The values of $,^M_k$ and $,^{\underline{N}}_{k} \equiv ,^N_k$ that have been previously computed must be modified according to Eq. (4.19) for

each bond $(k;\bar{k})$ linking two nodes $\vec{r}^M$ and $\vec{r}^N$ belonging to M and N, respectively. Hence, using the approximation described in Section 4.2, the common value of $,_k.\vec{r}^M/$ and $,_{\bar{k}}.\vec{r}^N/$ is given by

$$[,_I.\vec{r}^M;\vec{r}^N/]^2 = fi\left[,_k^M\right]^2 + [1-fi]\left[,_k^N\right]^2;$$

where $0 \le fi \le 1$. In many cases, choosing $fi = 0{:}5$ will be sufficient.

Given this new value of $,_k.\vec{r}^M/$ and $,_{\bar{k}}.\vec{r}^N/$, the coefficients $,_7.\vec{r}^M/$ and $,_7.\vec{r}^N/$ must be modified according to (4.24) and (4.25)

$$\left[,_7.\vec{r}^M/\right]^2 = \left[,_7^M\right]^2 + [1-fi]\sum_{k=1}^{n^M}\left\{\left[,_k^M\right]^2 - \left[,_k^N\right]^2\right\}$$

$$\left[,_7.\vec{r}^N/\right]^2 = \left[,_7^N\right]^2 - fi\sum_{k=1}^{n^N}\left\{\left[,_k^M\right]^2 - \left[,_k^N\right]^2\right\};$$

where n^M (resp. n^N) are the number of bonds, which connect node $\vec{r}^M$ (resp. $\vec{r}^N$) to medium N (resp. M).

Finally, it is important to point out that it is not necessary to compute the scattering elements $s_{kl}^M.\vec{r}/$, which describe the scattering process according to $S_k.\vec{r};t/ = \sum_{l=1}^7 s_{kl}^M.\vec{r}/E_l.\vec{r};t/\ k = 1;:::;7$ (Eq. (2.1)). Actually, due to Eq. (2.5), it is easy to show that the scattering process reads

$$S_k.\vec{r};t/ = ,_k^M.\vec{r}/\hat{}.\vec{r};t/ - E_k.\vec{r};t/; \qquad k = 1;:::;7: \tag{4.28}$$

Hence, given seven currents $E_k.\vec{r};t/$ incident at node $\vec{r}$ and at time t, one first computes $9.\vec{r};t/ = \sum_{k=1}^7 ,_k^M.\vec{r}/E_k.\vec{r};t/$ according to (2.2) and then $S_k.\vec{r};t/$ according to (4.28).

5. NUMERICAL EXAMPLES

To demonstrate the capability of the anisotropic wave automaton, we consider a circular particle (medium 1) immersed in a homogeneous isotropic medium (medium 2). The system is excited by a plane wave and the scattering pattern is recorded at the opposite side. First, the particle is chosen isotropic in order to compare the wave automaton results to known far-field patterns obtained using Mie theory. In the second example, the scattering properties of an anisotropic particle have been computed using the wave automaton. Finally, the scattered field of a collection of anisotropic particles is also presented.

5.1. Isotropic Scatterers

Medium 2 is characterized by its refractive index $n' = c_{\max}{=}c'$, where $c_{\max} = c_0{=}\sqrt{2}$. In the same way, the scatter is characterized by its refractive index $n = c_{\max}{=}c$ where $c = c_X = c_Y$. In the following example, $n' = 1{:}527$ and $n = 1{:}636$. Figure 6 displays the spatial map of the field amplitude at a fixed time when the field is stationary. Presenting the field amplitude instead of the intensity is convenient to display the small amplitude wavelets scattered far away from the particle. In this example, $k_2 R = 29{:}85$, where k_2 is the wave number in medium 2 and R is the radius of the scatterer. The physical values are $R = 2$ „m for $, = 0{:}64$ „m in vacuum in the case of light propagation. The corresponding numerical

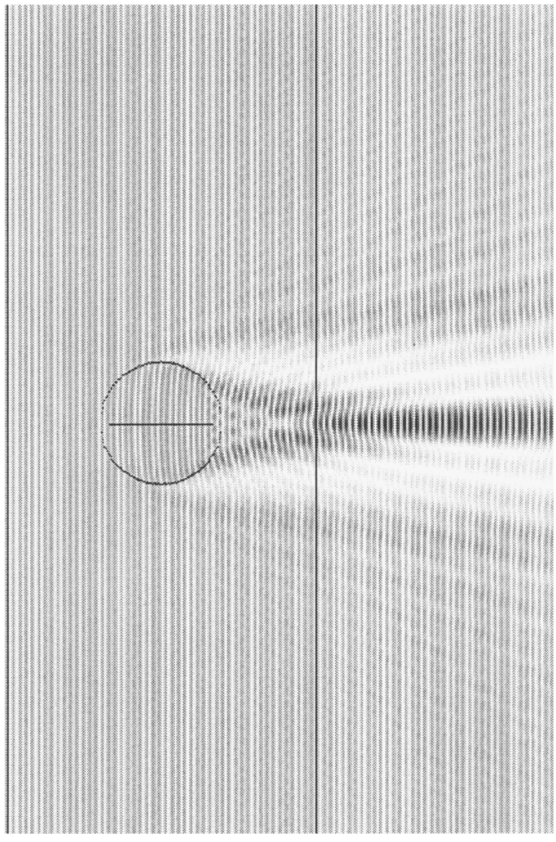

FIG. 6. Map of the field amplitude scattered by an isotropic disc. The system is excited by a plane wave propagating from the left to the right hand side. To compute the far-field intensity, the near field has been recorded along the vertical line drawn behind the scatterer.

values used in our simulations are $R = 44a$ and $\lambda_2 = 9.3a$, where λ_2 is the wavelength in medium 2 and a is the unit step of the hexagonal grid.

The near-field pattern obtained in this example has been recorded along the vertical line indicated in Fig. 6. Then, standard diffraction theory has been used to compute the far-field intensity along a circle having a large radius compared to the wavelength and the size of the particle. The result is compared in Fig. 7 with the analytical values provided by the Mie scattering theory in a two-dimensional geometry [19]. If we superimpose the two curves in Fig. 7, they cannot be distinguished from each other. To obtain a better comparison, the curves of Fig. 7 have been displayed in Fig. 8 using a logarithmic scale. Far-field intensities for particles with other radii R are also presented. For each radius R, the two curves computed with the wave automaton and with the Mie analytical results are superimposed. The agreement is excellent at the center of the curves but deteriorates at large angles. This effect is expected because of the finite size of the numerical box that contains the particle. For large observation angles, the computation of the far-field amplitude needs values of the near field close to the lateral boundaries of the system. Since presently a perfectly matched layer absorbing scheme is not available for the wave automaton, simple absorbing layers have been used to reduce wave reflection by the boundaries. Thus, near field values close to the boundaries are strongly disturbed. This results in the

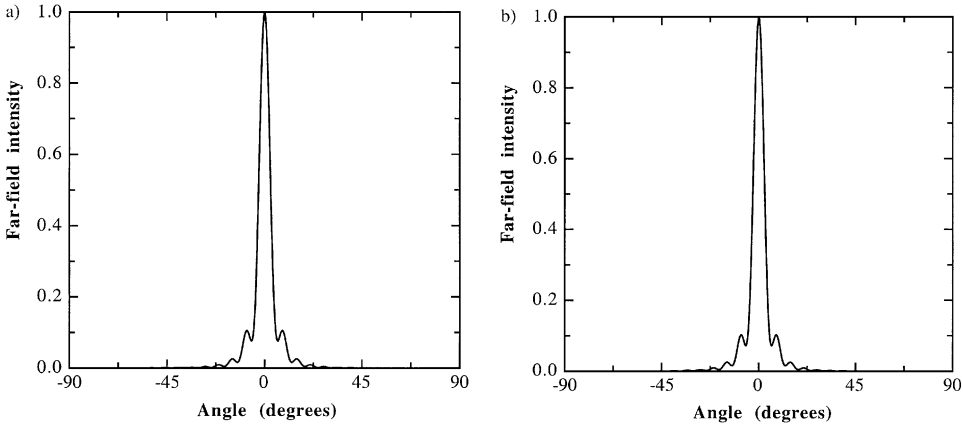

FIG. 7. (a) Far-field intensity computed from the near field displayed in Fig. 6. (b) Far-field intensity computed from the Mie scattering theory ($R = 2$ „m, , $= 0{:}64$ „m).

large drops of the wave automaton intensities near -90° and $+90^\circ$, which are clearly distinct from the Mie curves. However, the agreement, which is observed at the center of the curves for all particle radii, demonstrates that good accuracy can be obtained with the wave automaton.

5.2. Anisotropic Scatterers

Medium 2 is the same as in Section 5.1. We have also used the same value $k_2 R = 29{:}85$. The scatterer is now characterized by two different indices $n_X = 1{:}527$ and $n_Y = 1{:}744$. Such values are encountered for instance in liquid crystals.

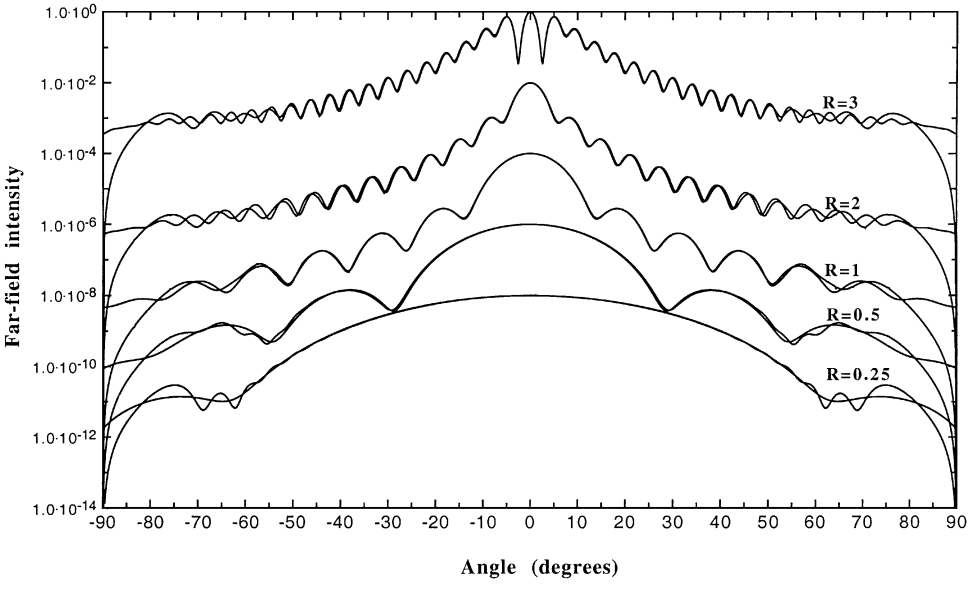

FIG. 8. Far-field intensities of scatterers with different radius R. „m) at , $= 0{:}64$ „m. For each radius R, the curves computed with the wave automaton and with the Mie analytical results have been superposed. The large drops observed near -90° and $+90^\circ$ belong to the wave automaton curves as explained in the text. For clarity of the figure, the different pairs of curves have been vertically shifted.

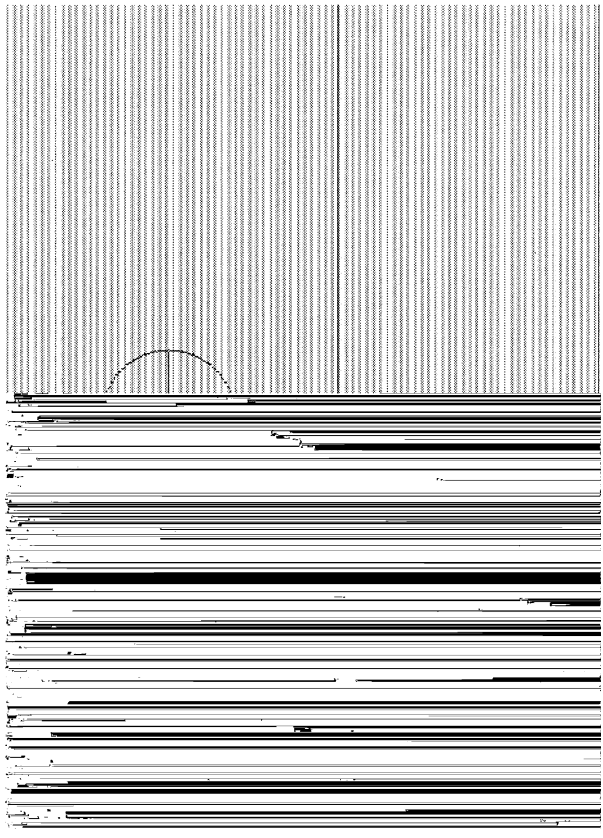

FIG. 9. Map of the field amplitude scattered by an anisotropic disc ($\mu = 0$). The direction of propagation corresponding to the largest index $n_y = n_Y = 1.744$ is indicated by a vertical line drawn inside the scatterer.

Three orientations μ of the principal axes X and Y have been chosen, $\mu = 0; \mu = \ldots = 4$, and $\mu = \ldots = 2$. Note that the indices n_X in medium 1 and n' in medium 2 have been chosen identical on purpose. When $\mu = 0; n_x = n_X = 1.527$ and $n_y = n_Y = 1.744$. As previously, the indices $x; y$ designate the absolute coordinate axes and $X; Y$ the principal axes of the scatterer. Hence, with an incident plane wave along the x axis, the wave propagates without scattering (Fig. 9). In contrast, scattering is observed when $\mu = \ldots = 2$ (Fig. 10). In this case $n_x = n_Y = 1.744$ and $n_y = n_X = 1.527$ inside the scatterer. We stress that both scatterers in Figs. 9 and 10 have the same indices. The only difference is the orientation of the principal axes. The asymmetry due to anisotropic scattering is clearly seen in the third example, where $\mu = \ldots = 4$ (Fig. 11). The corresponding far-field patterns are presented in Figs. 12 and 13. Unfortunately, in contrast with isotropic scatterers, we are not aware of analytical or experimental far-field patterns for 2D anisotropic scattering.

Finally, it is interesting to give a last example with several anisotropic scatterers characterized by the same indices $n_X = 1.527$ and $n_Y = 1.744$ (Fig. 14). In this example, the orientations of the principal axes are randomly chosen among the three values $\mu = 0; \mu = \ldots = 4$ and $\mu = \ldots = 2$. The field scattered by each particle as a function of μ is clearly illustrated. Such a situation is encountered for instance in polymer dispersed liquid crystals. Such materials are made of liquid crystal droplets randomly dispersed in a polymer matrix. Because the liquid crystal is in the nematic phase, each droplet behaves as a uniaxial medium. Such materials are known for their strong scattering properties when the droplets are randomly oriented.

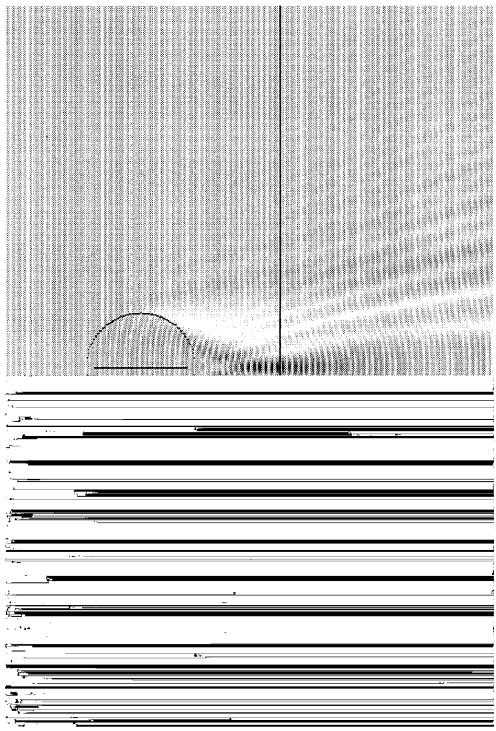

FIG. 10. Map of the field amplitude scattered by an anisotropic disc ($\mu = \ldots$=2). The direction of propagation corresponding to the largest index $n_x = n_Y = 1{:}744$ is indicated by a horizontal line drawn inside the scatterer.

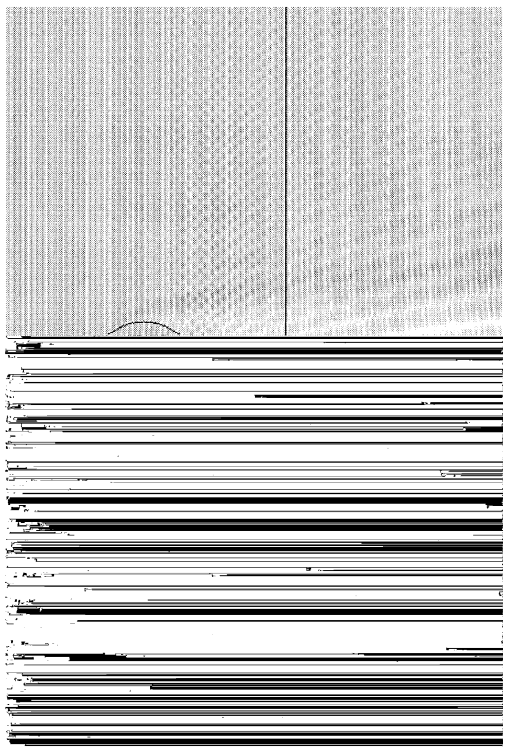

FIG. 11. Map of the field amplitude scattered by an anisotropic disc ($\mu = \ldots$=4). Inside the scatterer, the direction of propagation corresponding to the largest index $n_Y = 1{:}744$ is indicated by the oblique line.

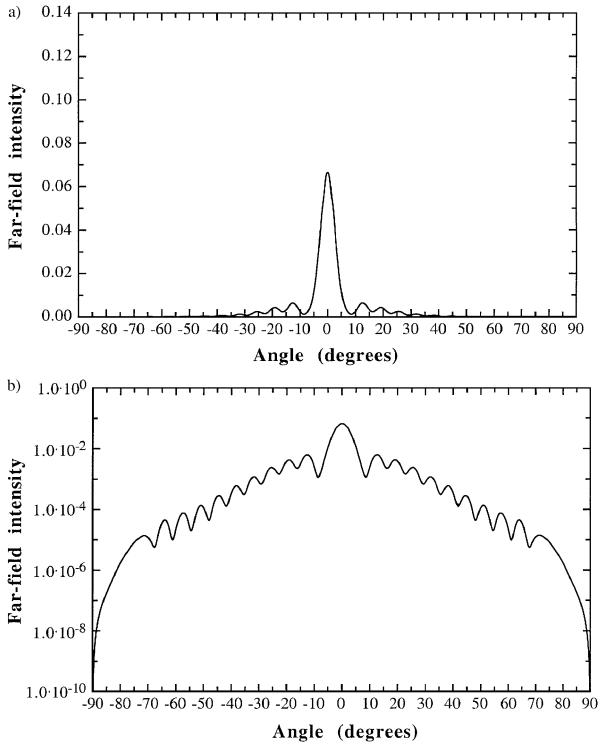

FIG. 12. Far-field intensity computed from the near fields corresponding to $\mu = \ldots = 2$ (Fig. 10): (a) linear vertical scale; (b) logarithmic vertical scale.

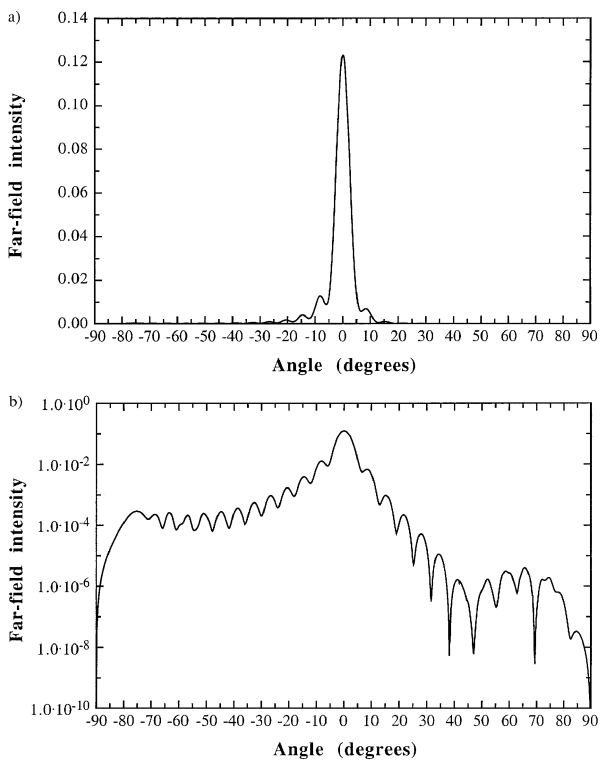

FIG. 13. Far-field intensity computed from the near fields corresponding to $\mu = \ldots = 4$ (Fig. 11): (a) linear vertical scale; (b) logarithmic vertical scale.

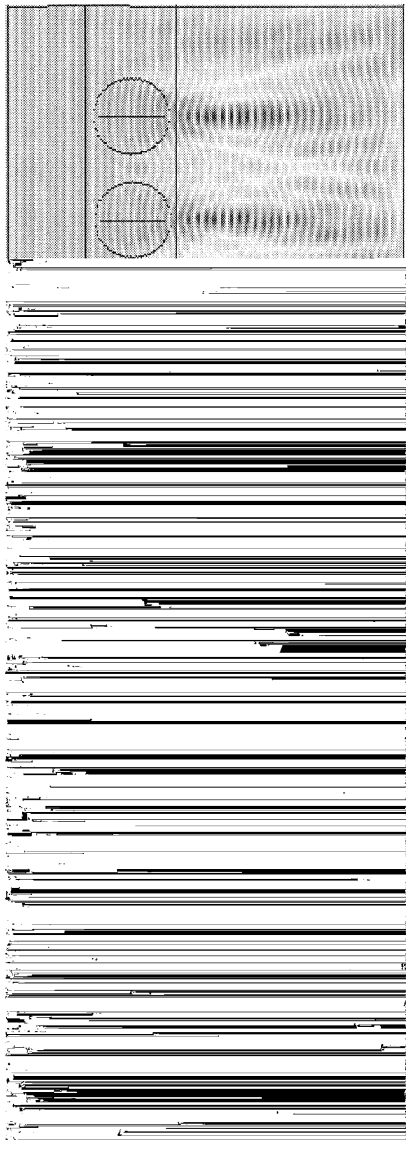

FIG. 14. Map of the field amplitude scattered by a collection of anisotropic particles. The system is excited by a plane wave propagating from the left- to the right-hand side. The direction of propagation corresponding to the largest index is indicated by a vertical line drawn inside each scatterer. In this example, $n_X = 1{:}527$, $n_Y = 1{:}744$, $R = 1$ „m, , $= 0{:}64$ „m.

6. CONCLUSION

In this paper, we have developed an extension of the wave automaton model [7] that has been recently introduced to describe scalar wave propagation in the time domain. It has been shown that using a hexagonal grid instead of the commonly used Cartesian grid naturally leads to the modeling of wave propagation in anisotropic media. The results of this model have been compared with known results using Mie theory. The introduction of a hexagonal grid is one of the original features of our model. A major consequence is to

avoid the interpolating schemes that are necessary with a Cartesian grid. We stress that this result is not limited to the wave automaton and is also valid for traditional finite-difference schemes. It is also worth noting that the scheme is unconditionally stable since the time evolution of the currents relies on a network of orthogonal matrices. Another original aspect of this work is to demonstrate that the complex case of anisotropic materials with arbitrary orientations can also be modeled by an approach based on a discrete Huygens' principle. Currently, our model is limited to 2D media. The next step is to extend these results to Maxwell and elastodynamics equations in 3D media.

ACKNOWLEDGMENTS

This work is currently supported by DGA Contract 97-406, by a CNRS grant, and by the GdR PRIMA.

REFERENCES

1. C. Vanneste, P. Sebbah, and D. Sornette, A wave automaton for time-dependent wave propagation in random media, *Europhys. Lett.* **17**, 715, (1992); **18**, 567 (1993) (Erratum).
2. P. Sebbah, D. Sornette, and C. Vanneste, A wave automaton for wave propagation in the time domain. I. Periodic systems, *J. Phys. I (France)* **3**, 1259 (1993); A wave automaton for wave propagation in the time domain. II. Random Systems, *J. Phys. I (France)* **3**, 1281 (1993).
3. P. Enders, Huygens' principle and the modelling of propagation, *Eur. J. Phys.* **17**, 226 (1996).
4. W. J. R. Hoefer, Huygens and the computer—A powerful alliance in numerical electromagnetics, *Proc. IEEE* **79**, 1459 (1991), and references cited therein.
5. N. R. S. Simons, G. E. Bridges, and M. Cuhaci, A lattice gas automaton capable of modeling three-dimensional electromagnetic fields, *J. Comput. Phys.* **151**, 816 (1999).
6. D. Sornette, O. Legrand, F. Mortessagne, P. Sebbah, and C. Vanneste, The wave automaton for time-dependent Schrödinger, classical wave and Klein–Gordon equations, *Phys. Lett. A* **178**, 292 (1993).
7. S. de Toro Arias and C. Vanneste, A new construction for scalar wave equations in inhomogeneous media, *J. Phys. I (France)* **7**, 1071 (1997).
8. B. Chopard, P. O. Luthi, and J.-F. Wagen, Lattice Boltzmann method for wave propagation in urban microcells, *IEE Proc. Microw. Antennas Propag.* **144**, 251 (1997).
9. B. Chopard and M. Droz, *Cellular Automata Modeling of Physical Systems* (Cambridge Univ. Press, Cambridge, UK, 1998), and references therein.
10. B. M. Boghosian and W. Taylor, Simulating quantum mechanics on a quantum computer, BU-CCS-970103 preprint quant-ph/9604035, talk presented at the PhysComp '96, Boston University, Boston, 1996.
11. D. Meyer, From quantum cellular automata to quantum lattice gases, USCD preprint quant-ph/9604003, 1996.
12. B. Shapiro, Renormalization group transformation for the Anderson transition, *Phys. Rev. Lett.* **48**, 823 (1982).
13. P. Freche, M. Janssen, and R. Merkt, Localization in nonchiral network models for two-dimensional disordered wave mechanical systems, *Phys. Rev. Lett.* **82**, 149 (1999).
14. J. Schneider and S. Hudson, The finite-difference time-domain method applied to anisotropic material, *IEEE Trans. Antennas Propagat.* **41**, 994 (1993).
15. J. Huang and K. Wu, A united TLM model for wave propagation of electrical and optical structures considering permittivity and permeability tensors, *IEEE Trans. Microwave Theory Tech.* **43**, 2472 (1995).
16. K. Kunz and R. Luebbers, *The Finite Difference Time Domain Method for Electromagnetics* (CRC Press, Boca Raton, FL, 1993).
17. A. Taflove, *Computational Electrodynamics: The Finite-Difference Time-Domain Method* (Artech House, Norwood, MA, 1995).
18. C. Christopoulos, *The Transmission Line Modelling Method* (IEEE Press, Piscataway, NJ, 1993).
19. H. C. van de Hulst, *Light Scattering by Small Particles* (Dover, New York, 1981).